Journal of Geoscience and Environment Protection, 2024, 12, 252-271
https://www.scirp.org/journal/gep
ISSN Online: 2327-4344
ISSN Print: 2327-4336

Remote Sensing and Geospatial Approach for Assessing the Impact of Automobiles on Air Quality, Case Study: Casablanca

Habiba El Alami El Kamouri[1], Rachid Essamoud[1], Mustapha Hakdaoui[2]

[1]Geosciences and Applications Laboratory, Faculty of Sciences Ben M'sik, The University Hassan II of Casablanca, Casablanca, Morocco
[2]Applied Geology, Geomatics and Environment Laboratory, Faculty of Sciences Ben M'sik, The University Hassan II of Casablanca, Casablanca, Morocco
Email: habiba.elalami@gmail.com, habiba.elalami1-etu@etu.univh2c.ma

How to cite this paper: El Alami El Kamouri, H., Essamoud, R., & Hakdaoui, M. (2024). Remote Sensing and Geospatial Approach for Assessing the Impact of Automobiles on Air Quality, Case Study: Casablanca. *Journal of Geoscience and Environment Protection, 12,* 252-271.
https://doi.org/10.4236/gep.2024.1211014

Received: October 11, 2024
Accepted: November 26, 2024
Published: November 29, 2024

Copyright © 2024 by author(s) and Scientific Research Publishing Inc.
This work is licensed under the Creative Commons Attribution International License (CC BY 4.0).
http://creativecommons.org/licenses/by/4.0/
Open Access

Abstract

Urban air pollution is a major challenge facing rapidly growing cities in the Middle East and North Africa (MENA) region, with vehicle emissions being a significant contributor. This study aims to analyze the spatial and temporal patterns of air pollutants, particularly nitrogen dioxide (NO_2), in Casablanca, Morocco, and investigate the relationship with urban development and transportation characteristics. By integrating satellite remote sensing data and Google Earth Engine (GEE) techniques, we provide a comprehensive assessment of air quality in Casablanca and demonstrate the value of using geospatial approaches for informing policymakers and urban planners. The results highlight seasonal variations in NO_2 levels, the identification of pollution hotspots, and the quantification of the influence of urban features and traffic on air quality. We discuss the implications of these findings for targeted interventions to improve air quality and the potential for expanding the methodology to other pollutants and cities in the region.

Keywords

Urban Air Pollution, Air Quality, Vehicle Emissions, NO_2, Satellite Imagery, Google Earth Engine

1. Introduction

Urban air pollution is a pressing environmental and public health concern, particularly in rapidly growing cities in the Middle East and North Africa (MENA) region. Vehicular emissions are a significant contributor to this problem, as the increasing number of automobiles and continued reliance on conventional fuels exacerbate air quality challenges (Seinfeld & Pandis, 2016; Lelieveld et al., 2015).

Casablanca, the largest city in Morocco, is no exception to this issue. As the country's economic and industrial hub, Casablanca has experienced rapid urbanization and motorization, leading to high levels of air pollution that pose risks to the health of its residents (Sekkat et al., 2012; Khoder, 2002). Understanding the spatial and temporal patterns of air pollutants in Casablanca and their relationship with urban development and transportation is crucial for informing policymakers and implementing effective mitigation strategies.

The use of satellite remote sensing and geospatial techniques, such as Google Earth Engine (GEE), has emerged as a powerful tool for monitoring and analyzing air quality in urban areas (Chudnovsky et al., 2014; Boloorani et al., 2018). These approaches provide a comprehensive, high-resolution view of air pollution dynamics, enabling the identification of hotspots, the quantification of trends, and the exploration of the underlying drivers.

This approach investigates the relationship between automobile traffic and air quality in Casablanca, Morocco. Using robust geospatial techniques and datasets such as Google Earth Engine (Gorelick et al., 2017), the study analyzes Sentinel-5P NO2 data (Veefkind et al., 2012), Sentinel-2 Land Use data (Drusch et al., 2012), ERA5 meteorological data (Hersbach et al., 2020), road network data, and traffic counts from 2019 to 2023. The analysis identifies seasonal trends, spatial hotspots of NO2 concentration, and the impact of urban development on air quality. This comprehensive approach leverages the capabilities of Google Earth Engine to integrate and analyze diverse datasets, providing valuable insights into the complex interactions between traffic, urbanization, and air quality.

This study aims to 1) analyze the spatial and temporal patterns of air pollutants, particularly nitrogen dioxide (NO_2), in Casablanca and 2) investigate the relationship between urban development, transportation, and air quality. By integrating satellite remote sensing data and GEE-based analyses, we demonstrate the value of using geospatial techniques for air quality monitoring and management in Casablanca and similar urban centers in the MENA region.

2. Materials and Methods

2.1. Study Area

Casablanca city (**Figure 1**) is located on Morocco's Atlantic coast, bordered by the ocean to the west and Settat and Ben Slimane provinces to the north, east, and south. The city covers 1140.54 km^2, with 18.8% (227.82 km^2) being urbanized. Urban areas doubled since the 1980s, growing from 100 km^2.

Casablanca, the largest city in Morocco, serves as the country's economic and industrial hub. With a population of over 3.3 million in the metropolitan area, Casablanca has experienced rapid urbanization and motorization, leading to significant air quality challenges (Sekkat et al., 2012).

The landscape features plains, plateaus, scattered hills, and a 98 km coastline, extending 22 km at Mansouria. The soil varies, with *Tirs* in rural areas and sandy soil along the coast. Rivers are minor, with Oued El Malleh, Oued N'fifikh, and Oued Hassar being the main ones. The city has 4000 ha of forests, mainly in Bouskoura.

The climate of Casablanca is a semi-arid one, with irregular rainfall, temperatures from 8˚C to 26˚C, and humidity levels always above 60%. Winds average 9 m/s from the northeast.

Geologically, Casablanca sits on sandy tuff formations with a shallow layer of soil. Hydrogeologically, groundwater is sparse and not highly vulnerable.

Hydrology: Urban development dried up Oued Bouskoura's lower course, but flooding remains a risk during heavy rains.

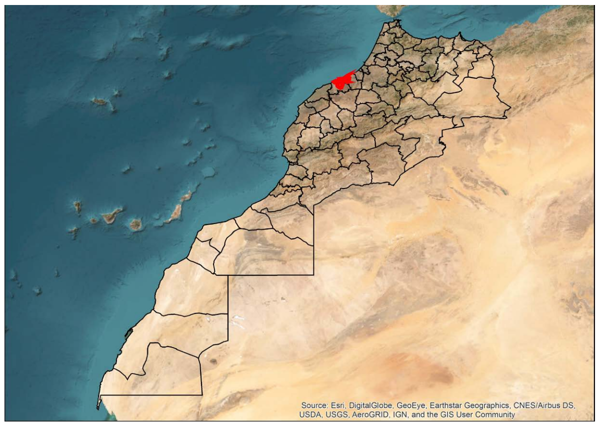

(a)

(b)

Figure 1. Location of the study area: (a) Morocco; (b) Casablanca city.

2.2. Data

This study utilized several satellite datasets accessed through Google Earth Engine (GEE): 1) Sentinel-5P NO_2 data, 2) Sentinel-2 Land Use Data, and 3) ERA5.

Other additional datasets were integrated into the analysis: 4) road network, and 5) traffic data.

2.2.1. Sentinel-5P NO_2 Data

The Sentinel-5 Precursor mission instrument acquires data pertinent to air quality assessment. The TROPOMI instrument, a multispectral sensor, records reflectance of wavelengths crucial for measuring atmospheric concentrations of ozone, methane, formaldehyde, aerosol, carbon monoxide, nitrogen oxide, and sulfur dioxide, as well as cloud characteristics at a spatial resolution of 0.01 arc degrees (https://developers.google.com/earth-engine/datasets/catalog/sentinel-5p).

The Sentinel-5P satellite provides high-resolution measurements of atmospheric nitrogen dioxide (NO_2) concentrations, which are used as a proxy for vehicle emissions and urban air pollution. The NO_2 data was retrieved and preprocessed using GEE.

Table 1. Key information about the Sentinel-5P.

Name	Units	Description
NO_2_column_number_density	mol/m^2	Total vertical column of NO_2 (ratio of the slant column density of NO_2 and the total air mass factor)
tropospheric_NO_2_column_number_density	mol/m^2	Tropospheric vertical column of NO_2
stratospheric_NO_2_column_number_density	mol/m^2	Stratospheric vertical column of NO_2
NO_2_slant_column_number_density	mol/m^2	NO_2 slant column density

a. https://developers.google.com/earth-engine/datasets/catalog/COPERNICUS_S5P_OFFL_L3_NO2#bands.

This dataset provides offline high-resolution imagery of NO_2 concentrations, available from 2018-06-28T10:24:07Z to 2024-09-28T20:22:15Z. and the period used in this study is from 2019 January to 2023 December.

Nitrogen oxides (NO_2 and NO) are significant trace gases in the Earth's atmosphere, present in both the troposphere and the stratosphere (**Table 1**). These compounds enter the atmosphere through anthropogenic activities (primarily fossil fuel combustion and biomass burning) and natural processes (wildfires, lightning, and microbiological processes in soils). In this context, NO_2 is utilized to represent concentrations of collective nitrogen oxides because during daytime, i.e., in the presence of sunlight, a photochemical cycle involving ozone (O_3) converts NO into NO_2 and vice versa on a timescale of minutes (https://developers.google.com/earth-engine/datasets/catalog/COPERNICUS_S5P_OFFL_L3_NO2#description).

2.2.2. Sentinel-2 Land Use Data

Sentinel-2 satellite imagery was used to derive urban development indicators, such as the Normalized Difference Built-up Index (NDBI), to analyze the relationship between urban features and air quality.

Sentinel-2, as shown in Table 2, is a wide-swath, high-resolution, multi-spectral imaging mission supporting Copernicus Land Monitoring studies, including the monitoring of vegetation, soil and water cover, as well as observation of inland waterways and coastal areas (https://developers.google.com/earth-engine/datasets/catalog/COPERNICUS_S2_SR_HARMONIZED#description).

Table 2. Key information about the Sentinel-2.

Name	Pixel Size	Wavelengh	
B1: Aerosols	60 m	443.9 nm (S2A)	442.3 nm (S2B)
B2: Blue	10 m	496.6 nm (S2A)	492.1 nm (S2B)
B3: Green	10 m	560 nm (S2A)	559 nm (S2B)
B4: Red	10 m	664.5 nm (S2A)	665 nm (S2B)
B5: Red Edge 1	20 m	703.9 nm (S2A)	703.8 nm (S2B)
B6: Red Edge 2	20 m	740.2 nm (S2A)	739.1 nm (S2B)
B7: Red Edge 3	20 m	782.5 nm (S2A)	779.7 nm (S2B)
B8: NIR	10 m	835.1 nm (S2A)	833 nm (S2B)
B8A: Red Edge 4	20 m	864.8 nm (S2A)	864 nm (S2B)
B9: Water vapor	60 m	945 nm (S2A)	943.2 nm (S2B)
B11: SWIR 1	20 m	1613.7 nm (S2A)	1610.4 nm (S2B)
B12: SWIR 2	20 m	2202.4 nm (S2A)	2185.7 nm (S2B)

b. https://developers.google.com/earth-engine/datasets/catalog/COPERNICUS_S2_SR_HARMONIZED#bands.

2.2.3. ERA5

ERA5-Land, as shown in Table 3, is a reanalysis dataset that provides a consistent view of the evolution of land variables over several decades at an enhanced resolution compared with ERA5.

Hourly wind speed and temperature data were obtained from ERA5-Land covering the study period (https://developers.google.com/earth-engine/datasets/catalog/ECMWF_ERA5_LAND_MONTHLY_BY_HOUR).

Table 3. Key information about the ERA5-Land.

Name	Units	Description
temperature_2m	K	Temperature of air at 2 m above the surface of land, sea or in-land waters. 2 m temperature is calculated by interpolating between the lowest model level and the Earth's surface, taking account of the atmospheric conditions.
u_component_of_wind_10m_min	m/s	Minimum u_component_of_wind_10m value each month.
u_component_of_wind_10m_max	m/s	Maximum u_component_of_wind_10m value each month.

Continued

v_component_of_wind_10m_min	m/s	Minimum v_component_of_wind_10m value each month.
v_component_of_wind_10m_max	m/s	Maximum v_component_of_wind_10m value each month.

c. https://developers.google.com/earth-engine/datasets/catalog/ECMWF_ERA5_LAND_MONTHLY_AGGR#band.

2.2.4. Road Network and Traffic Data

Road network was collected from Organizing Authority for Urban Transport of Greatest Casablanca Region. A total of 587 vehicle traffic counts have been incorporated into the road network, covering the entire study area. Of these, 370 counts distinguish between different vehicle types.

This dataset corresponds to the permanent traffic counts managed by The Regional Directorate of Equipment, Transport and Logistics (RDETL) of Casablanca. Unlike the earlier peak-hour counts, these figures represent Annual Average Daily Traffic (AADT), aggregated across both traffic directions. Each traffic count is georeferenced to a specific road network segment.

The dataset includes the following key fields:

- Type_CPT: indicates the type of traffic count, with a value of National Center for Road Studies and Research (NCRSR)of Morocco;
- AADT_2ways: represents the AADT volume, encompassing both directions of traffic flow on the corresponding road segment.

The following table (Table 4) presents additional data related to the structure of travel patterns used for the implementation of the model and provides detailed information on the data sources.

Table 4. Additional data of traffic road network.

Type of Data	Geographical Precision and Geolocation	Source
All-mode and mode-specific (PT, Bus, Tram, 2-wheelers, Private Car, Heavy Goods Vehicle) travel matrix during morning peak hour (2010), corresponding to households surveyed by ALG	OD by ZAT	ALG Household Survey 2011 (raw data with adjustment weights)

2.3. Methods

The following (Figure 2) are the key components of the methodology used in this study: 1) Temporal Analysis; 2) Spatial Analysis; 3) Land Use Regression.

2.3.1. Temporal Analysis

Time series decomposition was performed on the NO_2 data to identify seasonal patterns and long-term trends in air pollution levels.

In this proposed method, we begun by converting the unit mole/m^2 to micromol/m^2 for more representativity of the Total vertical column of NO_2 (ratio of the slant column density of NO_2 and the total air mass factor), after that, we used ee.Reducer.mean() function of GEE to generate temporal aggregation monthly average NO_2 for study period from 2019 to 2023.

2.3.2. Spatial Analysis

Spatial interpolation and hotspot detection methods were applied to the NO_2 data to map the distribution of air pollutants and identify pollution hotspots across Casablanca.

ee.Reducer.mean() function of GEE was also used to generate the image series of the average of netrogene_monthly for the study period.

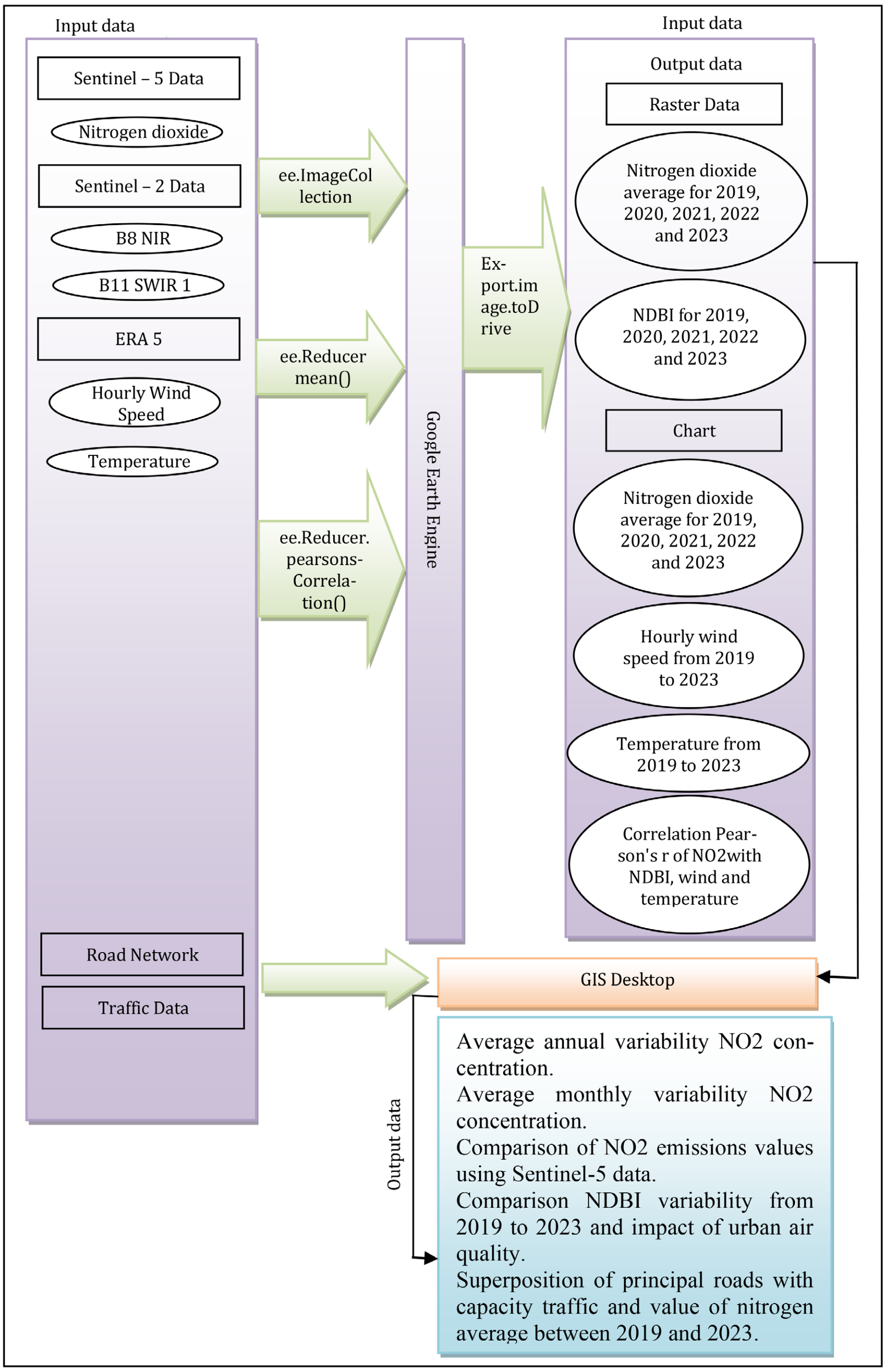

Figure 2. A systematic flowchart describing the process used for Assessing the Impact of Automobiles on Air Quality.

2.3.3. Land Use Regression

A regression modeling approach was used to quantify the influence of urban development indicators, traffic patterns, and meteorological factors like the impact of speed wind and temperature on NO_2 concentrations (Hoek et al., 2008; Jiang et al., 2020).

However, the methodology of our approach, which is completely built on the GEE cloud computing platform, began firstly by selecting a collection of images of the S2 L2 sentinel: 5 images per year; from 2019 to 2023. For each image, the Normalized Difference Built-up Index (NDBI) (Zha, Gao, & Ni, 2003) were calculated.

$$NDBI = \frac{B11 - B8}{B11 + B8}$$

where B8 is NIR, and B11 is SWIR 1. The NIR and SWIR bands are used to emphasize manufactured built-up areas, also this ratio is based to mitigate the effects of terrain illumination differences as well as atmospheric effects.

And use ee.Reducer.pearsonsCorrelation() function of GEE for correlation between NO_2 concentration and NDBI.

Secondly, use ERA5-Land on GEE to generate yearly charts of speed wind average and temperature average for each year, from 2019 to 2023, used ee.Reducer.mean() function of GEE, and ee.Reducer.pearsonsCorrelation() to correlate NO_2 concentration to speed wind, and correlate NO_2 concentration to temperature.

3. Results

The methodology described above has led to four levels of results: 1) Temporal Patterns of NO_2; 2) Spatial Distribution of NO_2; 3) Relationship between NO_2, Urban Development, and Traffic; and 4) Integration of Meteorological Data.

3.1. Temporal Patterns of NO_2

The temporal analysis of Sentinel-5P NO_2 data revealed distinct seasonal variations in air pollution levels across Casablanca. A time series decomposition showed consistent peaks in NO_2 concentrations during the winter months, potentially due to increased vehicle emissions and unfavorable meteorological conditions for pollutant dispersion.

From the charts (**Figure 3**), between 2019 and 2023, nitrogen dioxide (NO_2) concentrations exhibited peaks during the winter months. The highest concentrations were recorded in 2021, 2022, and 2023, showing a marked increase. However, a significant decrease in NO_2 concentrations was observed, from 93 μmol/m^2 in April 2019 to 78 μmol/m^2 in April 2020, and from 109 μmol/m^2 in October 2019 to 95 μmol/m^2 in October 2020. This significant reduction in NO_2 levels was observed, attributed to the COVID-19 lockdowns, which resulted in decreased vehicular traffic.

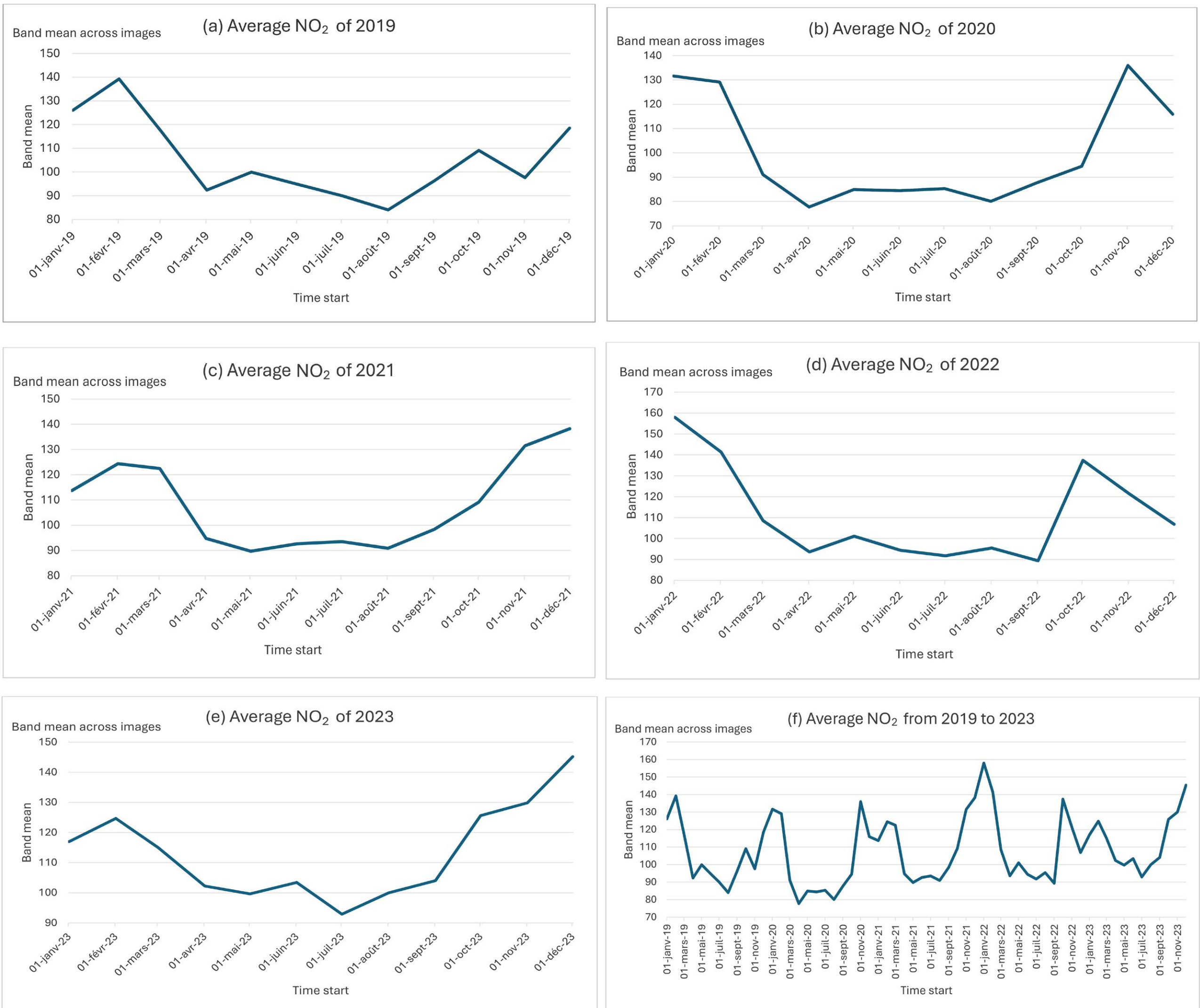

Figure 3. The temporal analysis of Sentinel-5P NO_2 data, from 2019 to 2023, on micromol/m².

3.2. Spatial Distribution of NO_2

The spatial analysis of NO_2 levels using GEE-based techniques identified several pollution hotspots within Casablanca. These hotspots were often located in areas with high traffic density, major transportation corridors, and industrial zones, highlighting the significant contribution of vehicular emissions and urban activities to air quality (Beirle et al., 2011).

The spatial analysis of NO_2 concentration levels (**Figure 4**) from 2019 to 2023 reveals that the highest concentrations, hotspots, were consistently recorded in the city center, an area characterized by the high traffic density of both private vehicles and heavy goods vehicles. This is primarily driven by the significant freight transport activity concentrated in this zone. Traffic density notably decreased in 2020 as a result of the COVID-19 pandemic but witnessed a rapid surge in 2023. This rebound reflects an increase in economic activity and vehicular traffic, as evidenced by the expansion of the vehicle fleet.

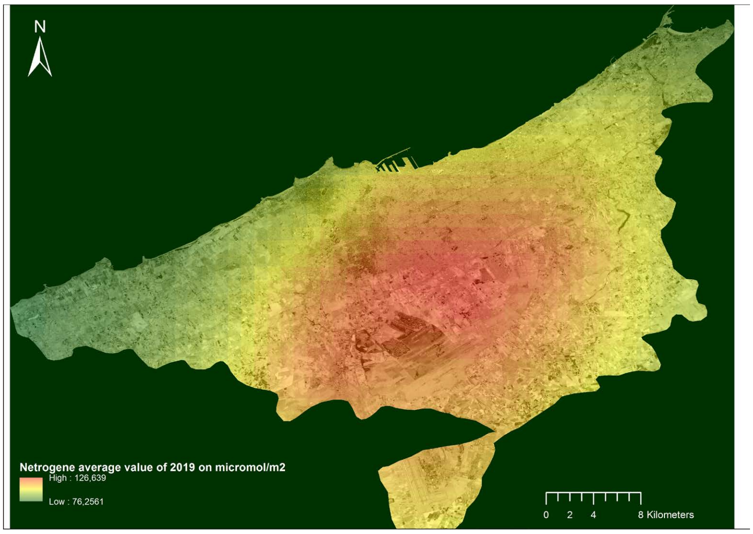
N
Netrogene average value of 2019 on micromol/m2
High : 126,639
Low : 76,2561
0 2 4 8 Kilometers

(a)

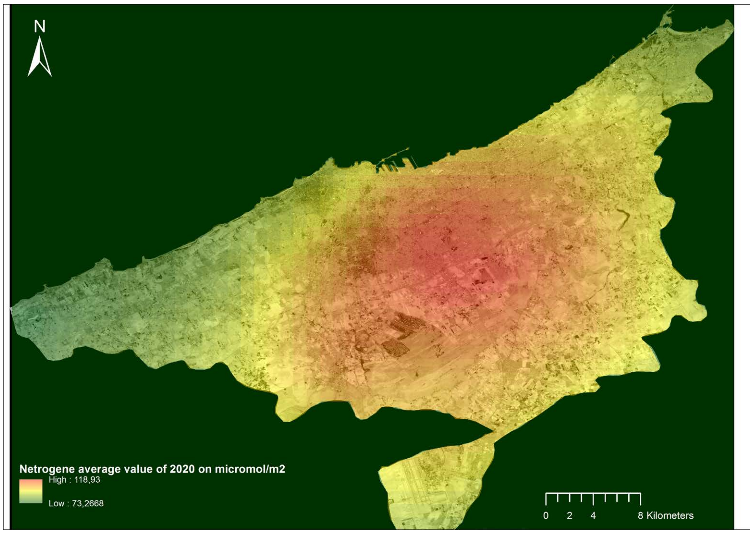
N
Netrogene average value of 2020 on micromol/m2
High : 118,93
Low : 73,2668
0 2 4 8 Kilometers

(b)

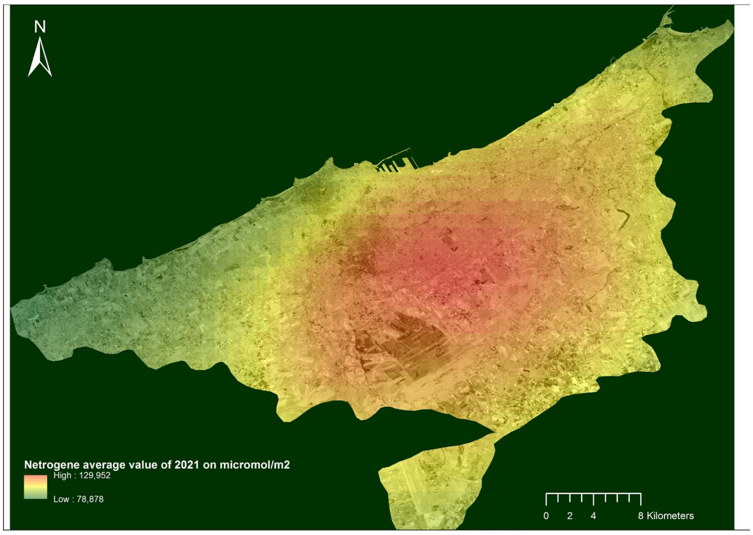
N
Netrogene average value of 2021 on micromol/m2
High : 129,952
Low : 78,878
0 2 4 8 Kilometers

(c)

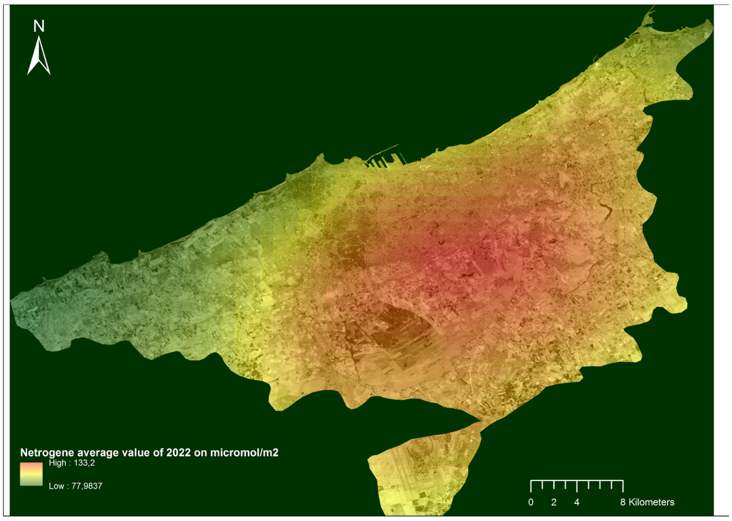

(d)

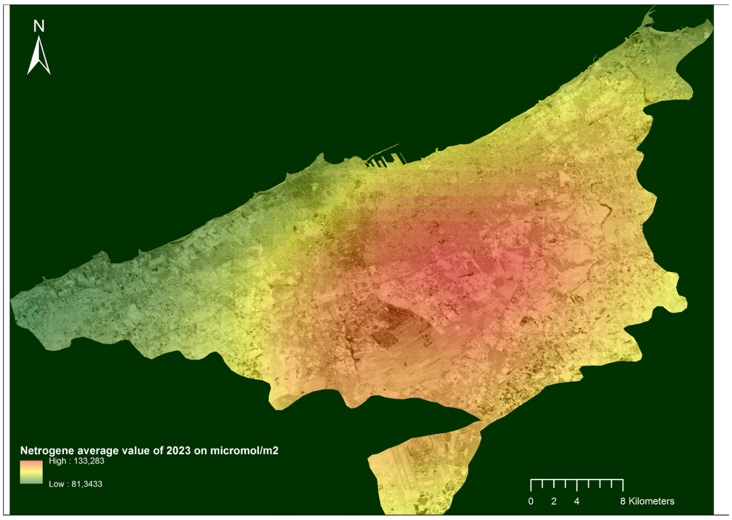

(e)

Figure 4. The spatial analysis of NO_2 levels of (a) 2019, (b)2020, (c) 2021, (d) 2022, and (e) 2023.

3.3. Relationship between NO_2, Urban Development, and Traffic

The land use regression analysis demonstrated a strong correlation between NO_2 concentrations and urban development indicators, such as the Normalized Difference Built-up Index (NDBI) (Figure 5). Areas with higher urban density and proximity to major roads exhibited elevated NO_2 levels, underscoring the impact of transportation and land use patterns on air pollution in Casablanca.

The chart of urban growth (Figure 6) depicts a substantial expansion of urban sprawl from 2002 to 2023, which has directly influenced increased mobility and is reflected in elevated air pollution levels, specifically the concentration of NO_2. This period exhibited a progressive increase in NO_2 concentrations extending towards the urban periphery. However, between 2019 and 2023, stabilization and subsequent reduction in urban growth levels were observed.

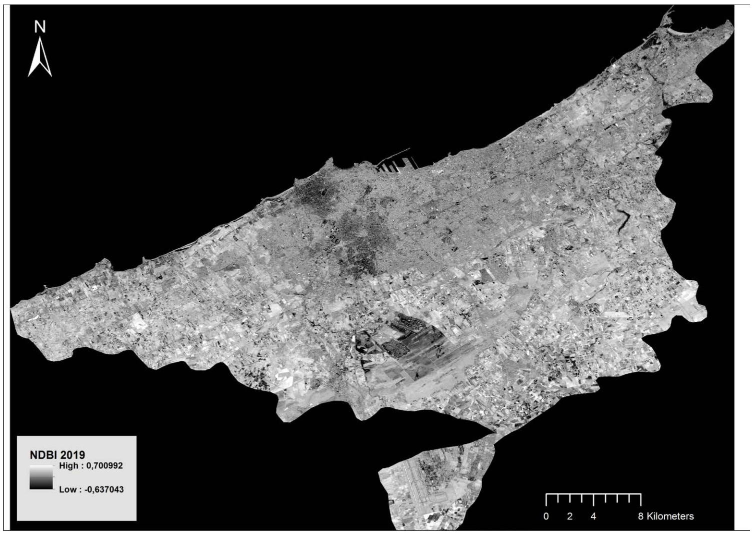
N
NDBI 2019
High : 0,700992
Low : -0,637043
0 2 4 8 Kilometers

(a)

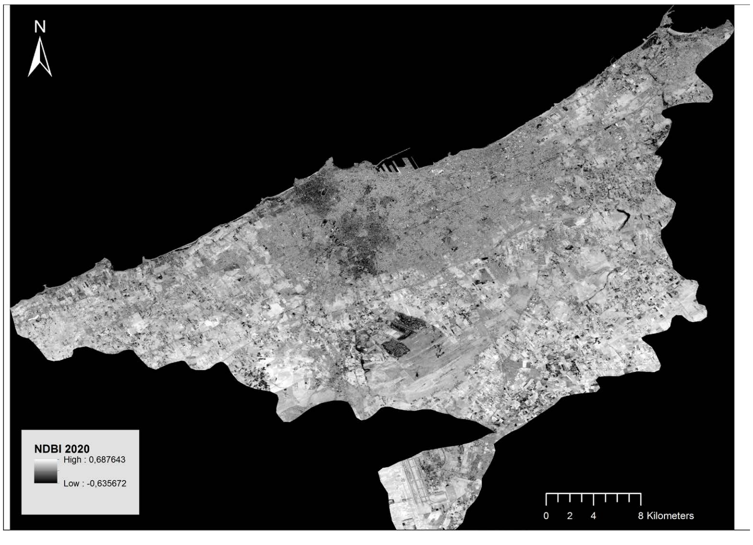
N
NDBI 2020
High : 0,687643
Low : -0,635672
0 2 4 8 Kilometers

(b)

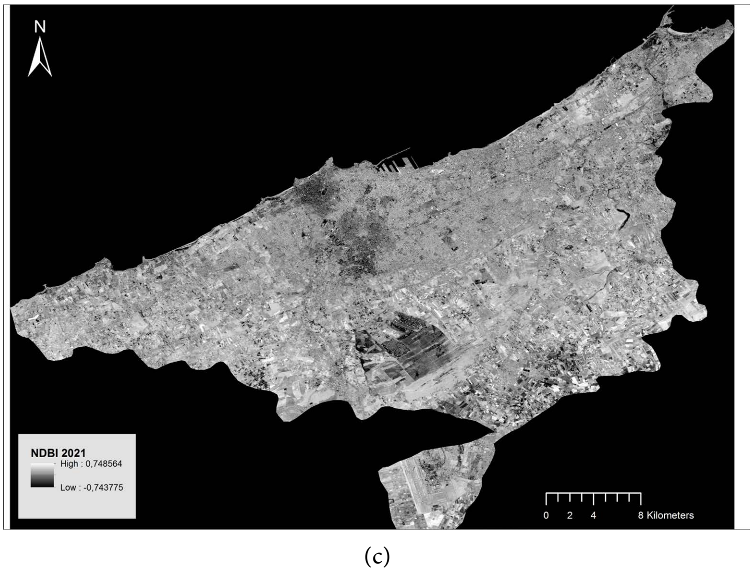
N
NDBI 2021
High : 0,748564
Low : -0,743775
0 2 4 8 Kilometers

(c)

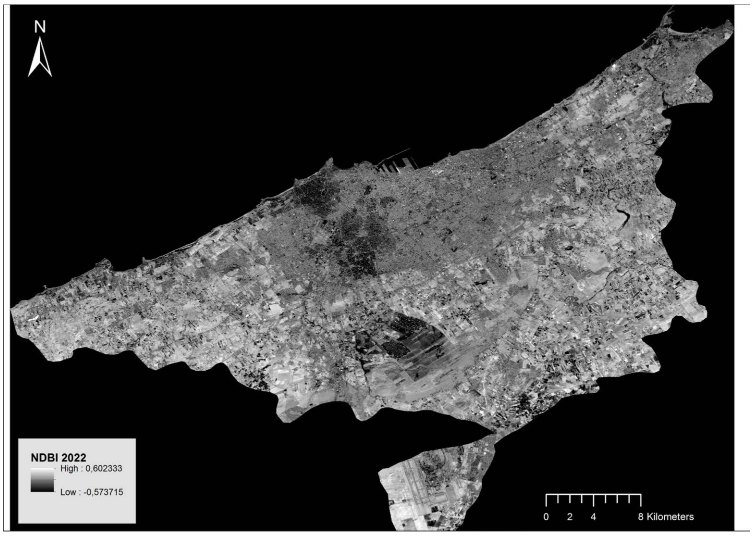

(d)

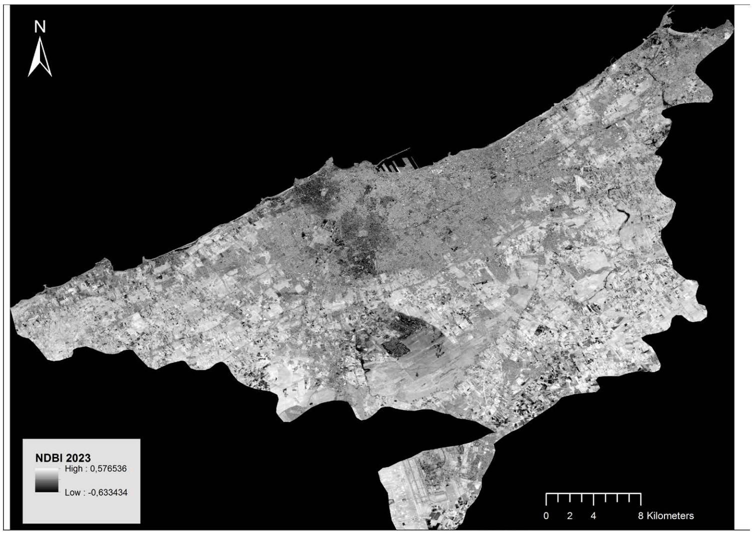

(e)

Figure 5. The spatial analysis of NDBI levels of (a) 2019, (b) 2020, (c) 2021, (d) 2022, and (e) 2023.

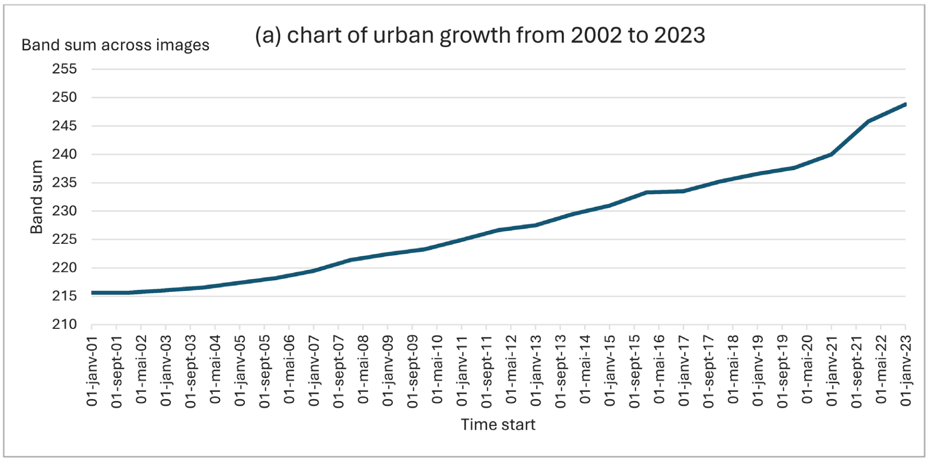

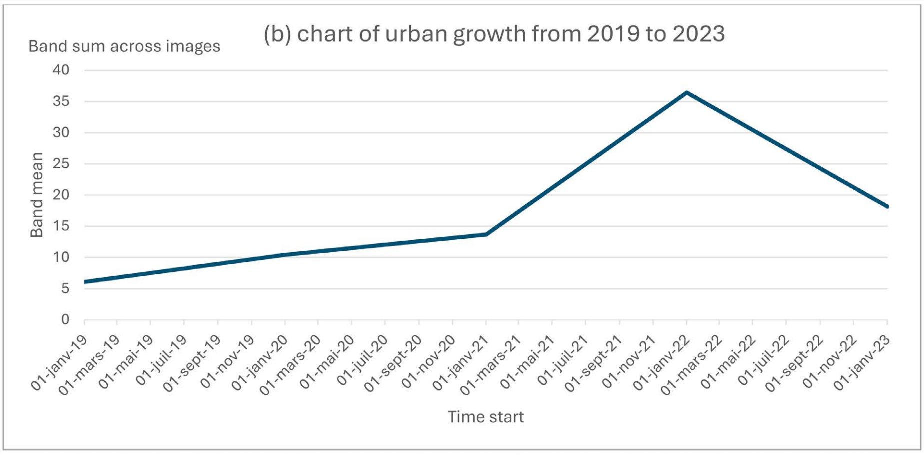

Figure 6. Chart of urban growth using Land Aerosol Optical Depth (AOD) from Terra & Aqua MAIAC Land Aerosol Optical Depth Daily 1 km.

Using Pearsons Correlation r from 2019 to 2023 (**Table 5**) demonstrates a weak negative correlation between NO_2 and NDBI in 2019. The negative sign indicates that as NDBI increases, indicating more built-up areas, and NO_2 concentrations levels tend to decrease. The magnitude of the correlation coefficient (−0.202) suggests a weak relationship. The *p*-value of 0 indicates that the correlation is statistically significant, meaning it is unlikely to be due to chance. These variables might show that while built-up areas (NDBI) are increasing, other factors like vehicular traffic could be contributing to the decrease in NO_2 concentrations levels. And in 2020 there is a very weak negative correlation between NO_2 concentrations and NDBI. The relationship is even weaker than in 2019. The *p*-value of 0 again indicates that the correlation is statistically significant. That reveal the reduction in NO_2 concentrations levels is more influenced by changes in traffic patterns rather than the built-up areas themselves. This could be due to lockdowns or reduced economic activities during the COVID-19 pandemic, which affected NO_2 emissions more than the built-up areas. However, in 2022, there is a very weak negative correlation between NO_2 concentrations and NDBI, similar to 2021 but slightly stronger, and the *p*-value of 0 indicates statistical significance. The slight increase in the correlation might indicate the changes in land use patterns or the introduction of new pollution control measures. These factors could be contributing to a more nuanced relationship between NDBI and NO_2 concentrations levels.

Table 5. Correlation Pearson's r and *P*-value between NO_2 concentration and NDBI from 2019 to 2023.

Years	Correlation Pearson's r	*P*-value
2019	−0.202	0
2020	−0.113	0
2021	−0.027	0
2022	−0.081	0
2023	0.105	0

In 2023 there is a weak positive correlation between NO_2 concentrations and NDBI. This is a change from the previous years where the correlation was negative. The positive sign indicates that as NDBI increases, NO_2 levels tend to increase as well. The magnitude of the correlation coefficient (0.105) suggests a weak relationship. The *p*-value of 0 indicates that the correlation is statistically significant. The increase in NO_2 levels is due to a combination of factors such as increased traffic, industrial activities, and possibly changes in land use that favor higher NO_2 emissions. This suggests that the relationship between NDBI and NO_2 is becoming more complex and influenced by a variety of environmental and socio-economic factors (Terry et al., 2024).

Figure 7 and **Figure 8** clearly illustrate the impact of traffic in principal roads and sum of origine destination displacement in air quality. The origine destination displacement is the effect of urban growth. Additionally, they illustrate the elevated levels of concentration that were found along major highways, including the A3 and A5 motorways. Lower concentrations were also shown in coastal areas, likely due to sea breezes and fewer emission sources.

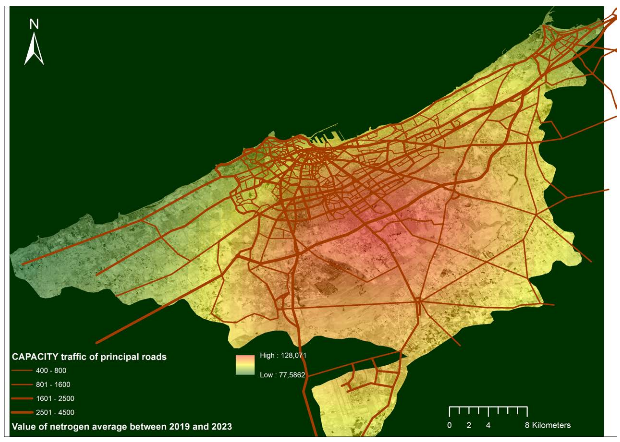

Figure 7. Superposition of principal roads with capacity traffic and value of nitrogen average between 2019 and 2023.

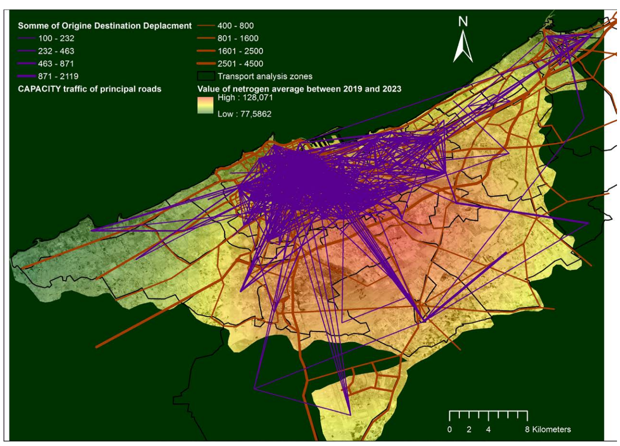

Figure 8. Superposition of sum of origine destination displacement and principal roads with capacity traffic and value of nitrogen average between 2019 and 2023.

For more accurate representation of traffic's impact on air pollution, the chart in Figure 9 shows the hourly traffic fluctuations and the pic of traffic were impact on air pollution.

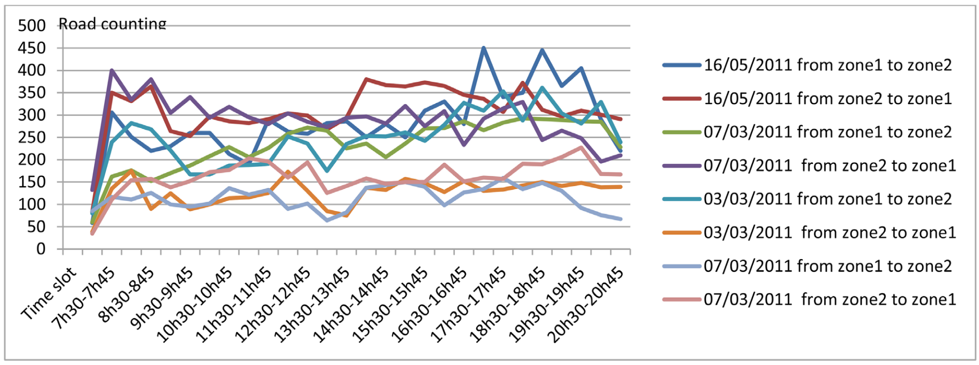

Figure 9. Chart of hourly traffic fluctuations. Source: ALG Household Survey 2011.

3.4. Integration of Meteorological Data

The incorporation of meteorological data (Figure 10) from the ERA5 reanalysis product revealed the influence of weather conditions on air quality in Casablanca. Factors such as temperature and wind patterns were found to play a significant role in the dispersion and accumulation of NO_2, contributing to the observed spatial and temporal variations.

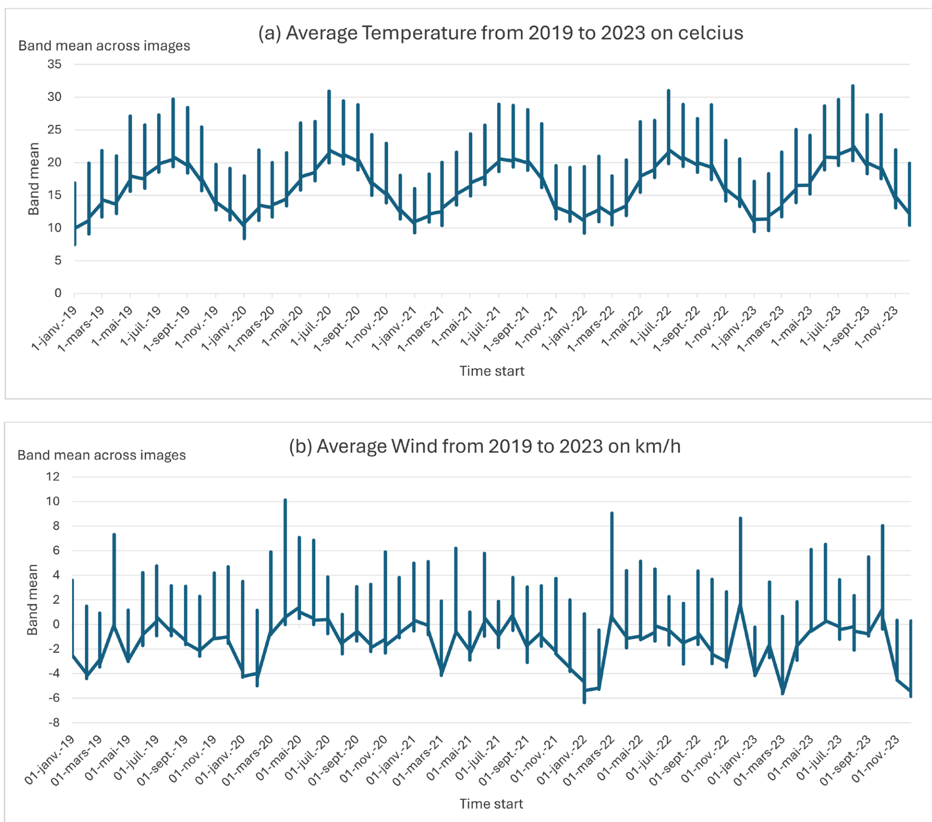

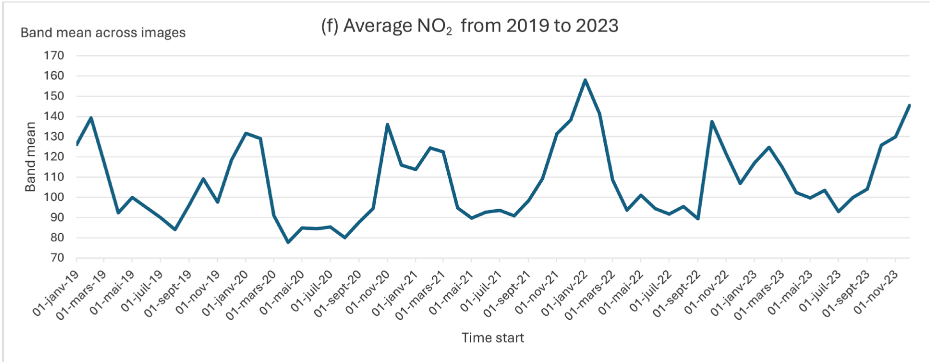

Figure 10. Measurement of average temperature and wind from ERA5.

The analysis of NO_2 concentrations levels in Casablanca, from 2019 to 2023 reveals significant correlations with meteorological variables such as temperature and wind. Including using Pearsons Correlation r (**Table 6**), the analysis demonstrated a consistent negative correlation is observed between NO_2 and temperature, indicating that higher temperatures are associated with lower NO_2 levels. This relationship has strengthened over the years, suggesting increased dispersion and chemical breakdown of NO_2 at higher temperatures (Jacob & Winner, 2009). The correlation between NO_2 and U-Wind (east-west wind component) is weak and positive, indicating that stronger east-west winds are associated with slightly higher NO_2 concentrations. This may be due to the transport of pollutants from urban or industrial areas (Seinfeld & Pandis, 2016). The correlation between NO_2 and V-Wind (north-south wind component) is strong and positive, highlighting the significant influence of north-south winds on NO_2 concentrations. This suggests that stronger north-south winds transport pollutants from high-emission areas, leading to increased concentrations downwind (Stull, 2012).

Table 6. Correlation Pearson's r and *P*-value between NO_2 concentration and meteorological variables: temperature, U-Wind, and V-Wind, from 2019 to 2023.

Years	Temperature		U-Wind		V-Wind	
	Correlation Pearson's r	*P*-value	Correlation Pearson's r	*P*-value	Correlation Pearson's r	*P*-value
2019	−0.302	0	0.067	0	0.500	0
2020	−0.288	0	0.094	0	0.467	0
2021	−0.361	0	0.163	0	0.473	0
2022	−0.434	0	0.270	0	0.684	0
2023	−0.477	0	0.308	0	0.633	0

The impact of automobile traffic on NO_2 concentrations levels can be inferred from the observed correlations. The strong positive correlation between NO_2 and V-Wind suggests that north-south winds may be transporting pollutants from high-traffic areas, in Casablanca, such as major roads and highways. This is supported by the findings that traffic flow and emissions are closely linked, and mitigating traffic congestion has a positive impact on air quality (Behera & Balasubramanian, 2016).

Moreover, the weak positive correlation between NO_2 and U-Wind indicates that east-west winds may also play a role in the transport of pollutants from traffic-heavy areas. This is consistent with the observation that vehicular emissions are a major source of urban air pollution (Behera & Balasubramanian, 2016). The increasing trend in the correlation between NO_2 and temperature over the years may also be influenced by changes in traffic patterns and urban development, which can affect the dispersion and chemical reactions of NO_2 (Eaton, 2022).

4. Discussion

The use of remote sensing and GEE-based approaches in this study provided a comprehensive, high-resolution view of air pollution dynamics in Casablanca, enabling the identification of hotspots, the quantification of trends, and the exploration of the underlying drivers. This methodological approach can be expanded to other pollutants as SO_2, PM_{10} and CO and cities in the MENA region, fostering a better understanding of air quality issues and informing evidence-based policymaking (Jerrett et al., 2017; Boloorani et al., 2018).

The reduction in NO_2 levels in 2020 had significant implications for air quality in urban areas, leading to temporary improvements in overall environmental conditions. However, as restrictions eased and economic activities resumed, NO_2 concentrations gradually increased, highlighting the strong correlation between human activities and air pollution. The experience during the COVID-19 pandemic underscored the potential for rapid environmental improvements when drastic measures are implemented, prompting discussions about sustainable urban planning and transportation policies for long-term air quality management (Tzortziou et al., 2022).

The weak and varying correlations between NO_2 concentrations levels and NDBI over the years demonstrate the relationship between urban development, as indicated by NDBI, and NO_2 pollution is complex and influenced by other factors such as industrial activity, traffic patterns, and meteorological conditions.

The strong correlations between NO_2 and meteorological variables, along with the significant influence of automobile traffic, demonstrate significantly that weather conditions and traffic management are crucial factors in air quality.

5. Conclusion

This study demonstrates the effectiveness of integrating satellite remote sensing data and Google Earth Engine techniques for assessing the impact of automobiles on air quality in Casablanca. The findings highlight the spatial and temporal patterns of nitrogen dioxide (NO_2), a key indicator of vehicle emissions, and reveal the significant influence of urban development, transportation, and meteorological factors on air pollution levels in the city.

The use of geospatial approaches enabled the identification of pollution hotspots, the quantification of trends, and the exploration of the underlying drivers of air quality, providing valuable insights for policymakers and urban planners to consider these factors when designing strategies to mitigate air pollution, and understand the complex interplay between urban development, meteorological conditions, traffic patterns, and NO_2 concentrations to effectively implement air quality management policies. This includes measures to reduce traffic congestion and promote cleaner transportation options. The health impact assessment underscored the need for targeted interventions to mitigate the risks posed by air pollution to the local population (Moltchanov et al., 2015).

The methodological framework developed in this study can be adapted and applied to other cities in the MENA region, contributing to a better understanding of air quality challenges and supporting the development of evidence-based strategies for improving urban environments. Continued collaboration between researchers, policymakers, and stakeholders is crucial for addressing the air pollution crisis and promoting sustainable development in rapidly growing urban centers like Casablanca.

Conflicts of Interest

The authors declare no conflicts of interest regarding the publication of this paper.

References

Behera, S. N., & Balasubramanian, R. (2016). The Air Quality Influences of Vehicular Traffic Emissions. In P. Sallis (Ed.), *Air Quality—Measurement and Modeling* (pp. 113-133). InTech Open. https://doi.org/10.5772/64692

Beirle, S., Boersma, K. F., Platt, U., Lawrence, M. G., & Wagner, T. (2011). Megacity Emissions and Lifetimes of Nitrogen Oxides Probed from Space. *Science, 333,* 1737-1739. https://doi.org/10.1126/science.1207824

Boloorani, A. D., Azizi, R., & Sabetghadam, S. (2018). Satellite-Based Air Quality Monitoring in the Middle East: A Utility Tool for Interdisciplinary Air Pollution Research. *MethodsX, 5,* 1207-1215.

Chudnovsky, A. A., Koutrakis, P., Kloog, I., Melly, S., Nordio, F., Lyapustin, A. et al. (2014). Fine Particulate Matter Predictions Using High Resolution Aerosol Optical Depth (AOD) Retrievals. *Atmospheric Environment, 89,* 189-198. https://doi.org/10.1016/j.atmosenv.2014.02.019

Drusch, M., Del Bello, U., Carlier, S., Colin, O., Fernandez, V., Gascon, F. et al. (2012). Sentinel-2: Esa's Optical High-Resolution Mission for GMES Operational Services. *Remote Sensing of Environment, 120,* 25-36. https://doi.org/10.1016/j.rse.2011.11.026

Eaton, D. (2022). *An Analysis of Automobile Traffic and Air Quality Data.* https://scholarworks.calstate.edu/downloads/5q47rv505?locale=en

Gorelick, N., Hancher, M., Dixon, M., Ilyushchenko, S., Thau, D., & Moore, R. (2017). Google Earth Engine: Planetary-Scale Geospatial Analysis for Everyone. *Remote Sensing of Environment, 202,* 18-27. https://doi.org/10.1016/j.rse.2017.06.031

Hersbach, H., Bell, B., Berrisford, P., Hirahara, S., Horányi, A., Muñoz-Sabater, J. et al. (2020). The ERA5 Global Reanalysis. *Quarterly Journal of the Royal Meteorological Society, 146,* 1999-2049. https://doi.org/10.1002/qj.3803

Hoek, G., Beelen, R., de Hoogh, K., Vienneau, D., Gulliver, J., Fischer, P. et al. (2008). A

Review of Land-Use Regression Models to Assess Spatial Variation of Outdoor Air Pollution. *Atmospheric Environment, 42,* 7561-7578. https://doi.org/10.1016/j.atmosenv.2008.05.057

Jacob, D. J., & Winner, D. A. (2009). Effect of Climate Change on Air Quality. *Atmospheric Environment, 43,* 51-63. https://doi.org/10.1016/j.atmosenv.2008.09.051

Jerrett, M., Donaire-Gonzalez, D., Popoola, O., Jones, R., Cohen, R. C., Almanza, E. et al. (2017). Validating Novel Air Pollution Sensors to Improve Exposure Estimates for Epidemiological Analyses and Citizen Science. *Environmental Research, 158,* 286-294. https://doi.org/10.1016/j.envres.2017.04.023

Jiang, N., Bao, Z., Zhou, H., Xin, J., & Hu, Y. (2020). Identifying Key Factors for Urban Air Pollution: Evidence from the Jing-Jin-Ji Region in China. *Sustainable Cities and Society, 54,* Article ID: 102005.

Khoder, M. I. (2002). Atmospheric Conversion of Sulfur Dioxide to Particulate Sulfate and Nitrogen Dioxide to Particulate Nitrate and Gaseous Nitric Acid in an Urban Area. *Chemosphere, 49,* 675-684. https://doi.org/10.1016/s0045-6535(02)00391-0

Lelieveld, J., Evans, J. S., Fnais, M., Giannadaki, D., & Pozzer, A. (2015). The Contribution of Outdoor Air Pollution Sources to Premature Mortality on a Global Scale. *Nature, 525,* 367-371. https://doi.org/10.1038/nature15371

Moltchanov, S., Levy, I., Etzion, Y., Lerner, U., Broday, D. M., & Fishbain, B. (2015). On the Feasibility of Measuring Urban Air Pollution by Wireless Distributed Sensor Networks. *Science of the Total Environment, 502,* 537-547. https://doi.org/10.1016/j.scitotenv.2014.09.059

Seinfeld, J. H., & Pandis, S. N. (2016). *Atmospheric Chemistry and Physics: From Air Pollution to Climate Change.* John Wiley & Sons.

Sekkat, N., Galindo, N., Yubero, E., Nicolás, J. F., Crespo, J., & Alastuey, A. (2012). Aerosol Pollution in the Urban Area of Rabat, Morocco. *Air Quality, Atmosphere & Health, 5,* 437-446.

Stull, R. B. (2012). *An Introduction to Boundary Layer Meteorology.* Springer Science & Business Media.

Terry, B., Kremer, P., Goldsmith, S. T., & Shakya, K. M. (2024). Land Use Regression Model to Predict Nitrogen Dioxide in the Greater Philadelphia Area. *Atmospheric Pollution Research.* https://doi.org/10.1016/j.apr.2024.102339

Tzortziou, M., Kwong, C. F., Goldberg, D., Schiferl, L., Commane, R., Abuhassan, N. et al. (2022). Declines and Peaks in NO_2 Pollution during the Multiple Waves of the COVID-19 Pandemic in the New York Metropolitan Area. *Atmospheric Chemistry and Physics, 22,* 2399-2417. https://doi.org/10.5194/acp-22-2399-2022

Veefkind, J. P., Aben, I., McMullan, K., Förster, H., de Vries, J., Otter, G. et al. (2012). TROPOMI on the ESA Sentinel-5 Precursor: A GMES Mission for Global Observations of the Atmospheric Composition for Climate, Air Quality and Ozone Layer Applications. *Remote Sensing of Environment, 120,* 70-83. https://doi.org/10.1016/j.rse.2011.09.027

Zha, Y., Gao, J., & Ni, S. (2003). Use of Normalized Difference Built-Up Index in Automatically Mapping Urban Areas from TM Imagery. *International Journal of Remote Sensing, 24,* 583-594. https://doi.org/10.1080/01431160304987